Investigating Safety of Evasion Maneuver Choices by Human-Driven Vehicles in Response to High-Density Truck Platoons Near Freeway Diverging Areas*

Zhili Wei, Chuan Xu, Kaan Ozbay, Yufeng Yang, Hong Yang, Fan Zuo, Di Yang and Chuanyun Fu

Abstract — **High-Density Truck Platoons (HTPs) introduce new safety challenges for Human-Driven Vehicles (HDVs) near freeway diverging areas due to their extensive spatial and temporal occupancy. When navigating around an HTP, HDVs approaching off-ramps face two Evasion Maneuver Choices (EMCs): Platoon Front Overtaking (PFO) and Platoon Back Evading (PBE). To evaluate EMCs safety, we conducted driving simulation tests in scenarios with short, medium, and long distances of releasing. We used trajectory data to derive Anticipated Collision Time (ACT) and other behavior and safety metrics. A generalized extreme value (GEV) model based on ACT was utilized to evaluate the crash risk during the lane-changing process to evade the HTP. The results indicated that in the short scenario, the crash risk for PFO is higher, while in the medium scenario, the crash risk for both ACPs is roughly equal. The long scenario sees PBE as the riskier behavior. In addition, the crash risk notably decreases when transitioning from short to medium scenarios, regardless of the selected EMCs. These findings have important implications for the development of lane-changing assistance devices for HDVs and safety-oriented lane management strategies near freeway diverging areas.**

I. Introduction

A notable application of autonomous and cooperative driving technologies is in the formation of High-Density Truck Platoons (HTPs), an innovative concept that connects multiple trucks at a minimal inter-vehicle distance to form a convoy. This configuration leverages the vehicular network and automated driving control system to significantly reduce air drag [1], leading to notable benefits in energy conservation and lower carbon emissions [2, 3]. While the technical feasibility of HTPs is well-documented in the literature [4], such as Vehicle-to-Vehicle Communication, Adaptive Cruise Control, Autonomous Emergency Braking, Automated Lane Keeping, there is a notable research gap regarding their safety implications, particularly in scenarios involving Human-Driven Vehicles (HDVs). Given the gradual adoption of Autonomous Vehicles (AVs), it is anticipated that mixed traffic conditions involving both AVs and HDVs will persist for a considerable period [5]. The safety impact of HTPs on HDVs in this mixed scenario, thus remains an important, yet largely unexplored, area of research.

Diverging areas on freeways are characterized by a high demand for lane changing [6]. In these zones, vehicles that are intending to exit the freeway must shift from the central lanes to the exit ramp's designated lane. This mandatory lane switching necessitates a change in speed to ensure a safe exit, leading to a heterogeneity in both lateral and longitudinal vehicle movement. This variation in movement can disrupt the flow of mainline traffic, potentially causing conflicts and even collisions. Historical crash data highlights that even in the absence of HTPs, these diverging areas on freeways are particularly prone to accidents[6-8]. The introduction of HTPs further complicates this situation due to their prolonged spatial and temporal occupancy and the visual obstruction they cause for other drivers. In this situation, the driver has two Evasion Maneuver Choices (EMCs) in response to HTP: Platoon Front Overtaking (PFO) and Platoon Back Evading (PBE). Understanding the risk associated with each EMC is crucial, as it can guide drivers to make safer and more informed decisions.

In an effort to address the existing research gap, this study seeks to evaluate the safety of EMCs when HDVs interacting with HTP in the vicinity of freeway diverging areas. We conducted a driving simulator experiment with thirty participants, featuring a configuration of a leading vehicle, a participant-driven main vehicle, a vehicle following the main vehicle, and an HTP. Participants in the experiment were instructed to follow the leading vehicle, which was driving alongside an HTP until the leading vehicle changed lanes. The distance from the point where the leading vehicle changed lanes to the exit ramp is referred to as the Distance of Releasing (DR) in this study. This DR can provide insight into the difficulties associated with mandatory lane changing near freeway exits. We tested three scenarios with different DRs, short DR scenario (300m, 400m) medium DR (500m, 600m), long DR (700m, 800m). Throughout the experiment, the vehicle trajectory and vehicle dynamics such as speed, accelerate for all vehicles were recorded for further analysis.

Based on the experimental data, we identified the stable car following stage and the Mandatory Lane Change Stage (MLCS) using the Gaussian Mixture Model (GMM). For the

*Research supported by C2SMART, a Tier 1 University Transportation Center at New York University, Sichuan Science and Technology Program (2021YJ0042), and the Key Laboratory of Road and Traffic Engineering of the Ministry of Education, Tongji University (K202001).

Zhili Wei, Chuan Xu, and Yufeng Yang are with the School of Transportation and Logistics, Southwest Jiaotong University, Chengdu, Sichuan, China (e-mail: weizhili@my.swjtu.edu.cn, xuchuan@swjtu.edu.cn, yangyufeng@my.swjtu.edu.cn).

Kaan Ozbay, Chuan Xu and Fan Zuo are with the C2SMART Center, Department of Civil and Urban Engineering, Tandon School of Engineering, New York University, Brooklyn, NY 11201, USA (e-mail: kaan.ozbay@nyu.edu, cx514@nyu.edu, fz380@nyu.edu).

Hong Yang is with the Department of Electrical and Computer Engineering, Old Dominion University. (e-mail: hyang@odu.edu).

Di Yang is with the Department of Transportation & Urban Infrastructure Studies, Clarence M. Mitchell, Jr. School of Engineering, Morgan State University. (e-mail: di.yang@morgan.edu)

Chuanyun Fu is with the School of Transportation Science and Engineering, Harbin Institute of Technology, and the Department of Civil Engineering, University of British Columbia. (e-mail:fcy1128@mail.ubc.ca)

MLCS, a series of safety surrogate measures are computed and a crash risk model based on Extreme Value Theory (EVT) was developed to quantify the driving risk of the main vehicle in different EMCs and scenarios.

The experimental design of driving simulation, indicator analysis and modelling techniques are described in Section II. Section III provides a specific analysis of the modelling results and crash risk. Section IV discusses the study findings, and the conclusions are presented in Section V.

II. Methodology

A. *Design and Development of Driving Simulation Experiments*

This study employed a fixed-base driving simulator for data collection. The simulator was equipped with a full-sized chair, steering wheel, and accelerator and brake pedals, mimicking the control features of a real vehicle. The three-dimensional simulated road environment was projected onto three screens in front of the driver, each with a resolution of 1920×1080, affording a 210-degree forward field of view. To enhance the immersive experience, left and right audio systems were utilized to simulate engine, road, and traffic noises, providing an auditory environment that mimics real-world driving conditions. The simulation software used for the experiment was SCANeR Studio, version 1.8.28.

Figure 1. Driving simulator and 3-D road environment.

We recruited thirty drivers to participate in the experiment. Prior to the experiment, each driver provided informed consent, completed a questionnaire capturing basic demographic information and took a 5-min test drive under the guidance of a lab assistant to ensure they could get familiar with the simulator. The participant group consisted of 17 men and 13 women, aged between 22 to 50 years, with a mean age of 30.44 years and a standard deviation of 8.11 years. All participants possessed a valid driving license, indicating they were legally qualified to operate a vehicle. The driving experience among participants varied, with a mean of 7.17 years and a standard deviation of 5.86 years.

The experiments were conducted using a simulation of a real-world section of the Chengdu 4th Ring Freeway. This section extends from 6 kilometers before Exit ramp 67 to 1 kilometer beyond the same exit ramp, also known as the Pidu exit. The simulated section includes a 150-meter off-ramp and a 200-meter deceleration lane leading to the ramp. The construction of the simulated scene utilized software tools such as SCANeR Studio, 3DS Max, and Open Street Maps. These tools were used to create the road alignment, surface, markings, and environmental objects. Additional features such as traffic signs and barrels were also incorporated to provide a realistic driving environment. The experimental road section is 7 kilometers in length with a speed limit of 120 kilometers per hour. It features three lanes in each direction, each with a width of 3.75 meters, closely resembling the actual physical specifications of the Chengdu 4th Ring Freeway.

The following experimental scenario was established for this study: a participant-driven vehicle, designated as the Main Vehicle (MV), headed towards Pidu, while a leading vehicle (LV) maintained its position on the same lane in front of the MV. As the MV approached the off-ramp, it encountered a HTP consisting of 10 trucks with 2.5m inter-vehicle spacing, occupying the rightmost lane (refer to Figure 2 (a)). At a specific location, the LV changed lanes to the left, freeing the space ahead of the MV (Figure 2 (b)). This change allowed the MV driver to decide the optimal timing and EMC (Figure 2 (c)(d)) to evade the HTP and transition onto the off-ramp. To measure the potential risk of rear-end collisions, each experiment also included a Rear Vehicle (RV) that followed the MV. Throughout the experiment, the RV was programmed to stay in its lane and consistently maintain a target time gap of 2.5 seconds behind the MV. LV, MV and RV occupied the second lane from the right. Except the RD, other conditions were consistently maintained across all experiments.

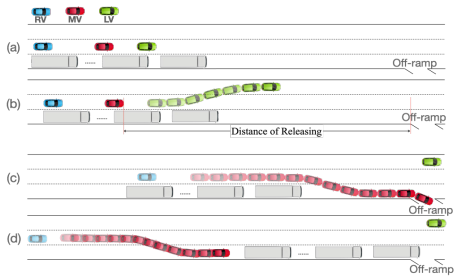

Note: (a) LV is leading the MV; (b) LV lane changing process and remaining distance; (c) EMC 1: Platoon Front Overtaking; (d) EMC 2: Platoon Back Evading.

Figure 2. Illustration of experimental design.

The parameters for the HTP were set as follows: the overall length of the platoon was 92.8 meters, each individual truck measured 7.0 meters, the inter-vehicle spacing was 2.5 meters, and the platoon traveled at a speed of 90 km/h. Previous studies have reported Time Headway (THW) values typically ranging between 0.3 and 1.5 seconds [9-11], with some research specifying a THW of 0.3 seconds for high-density platoon scenarios [12-14]. To emulate the characteristics of an HTP, our study set the inter-vehicle THW to approximately 0.38 seconds. In each experimental scenario, the timing for the LV lane change was adjusted according to predefined DR (refer to Figure 2b), set at three scenarios: short scenario (300m, 400m) medium scenario (500m, 600m), long scenario (700m, 800m). Each participant completed six trials, with each trial taking roughly 4 minutes to complete. Upon reaching the HTP, the LV keeps the same speed as the platoon and maintained a parallel course for a certain period. The LV keeps a distance of 24m from the head of the first truck in the HTP before it changes its lane to the left.

B. Dataset and Indicators

This study gathered driving data from a total of 180 driving simulation tests, which were performed by thirty different drivers, each conducting six tests (30 x 6=180 tests). However, data from three tests had to be discarded due to technical malfunctions with the equipment. The collected data included vehicle trajectory, speed, and acceleration for all vehicles involved. The distance between vehicles was calculated based on the trajectory data. The experiment consisted of two stages: the car following stage and the Mandatory Lane Changing Stage (MLCS). As the latter stage presents a more complex interaction and increased risk, our study focused solely on the risk during the MLCS. Consequently, it was crucial to clearly identify the MLCS for subsequent data analysis. However, given that the influence of the HTP varied among different tests, a fixed time window wasn't suitable for selection. Instead, drawing inspiration from Zhao's study (16), we incorporated the GMM to identify the MLCS.

Four Driving Performance Indicators (DPIs) and four Surrogate Safety Measures (SSMs) were computed as the covariates to build the EVT model. The four DPIs are speed, acceleration, Distance to Ramp (D2R), and Distance to the Platoon Center (DPC). The SSMs include Anticipated Collision Time (ACT), Acceleration Noise, Deceleration Rate to Avoid Collision (DRAC) and Time Extended ACT (TE-ACT).

D2R: D2R is the instantaneous measurement reflecting the distance between the current location of the MV and the off-ramp (see Figure 3 (a)).

DPC: the distance to the center of the HTP. When the MV is behind the HTP center of, DPC is positive (see Figure 3 (b)), and when the MV is ahead of the HTP center, DPC is negative (see Figure 3 (c)).

ACT: In this study, we require an indicator not only to measure the risk of a forward collision but also the risk of lane changing. Traditional conflict indicators, such as TTC and PET, are not suitable in this context. A two-dimensional extension of TTC that can reflect the crash risk corresponding to different crash types [15]. For the two different EMCs, the ACT between the MV and the vehicle which has the maximum crash risk with the MV is calculated. Specifically, for the PFO (Figure 2 (c)), the ACT between the MV and the head of HTP was calculated; in the PBE (Figure 2 (d)), the ACT between the RV and the MV was calculated.

Acceleration Noise: Acceleration noise is the standard deviation of acceleration during the MLCS.

DRAC: DRAC is a widely used SSI and indicates the minimum deceleration required for a following vehicle to avoid a crash with a leading vehicle [16]. Generally, a larger DRAC represents a more dangerous driving condition. In the experiment, there are many vehicles, the same as ACT, the DRAC which capture the riskiest situation is calculated. In PFO, the DRAC was calculated for the MV (following vehicle) and the first truck of the HTP (leading vehicle). In PBE, the DRAC was calculated for the RV (following vehicle) and the MV (leading vehicle).

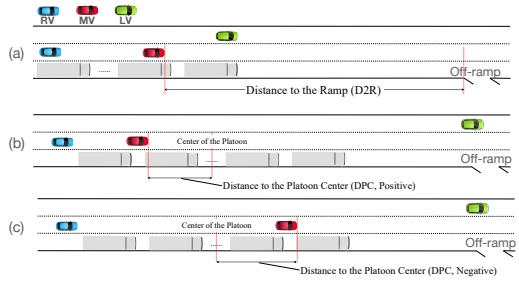

Figure 3. The illustration of the D2R and DPC.

TE-ACT: The cumulative time that the ACT is below the threshold. The greater the TE-ACT reflects a higher exposure to the dangerous driving situation. Refers to the studies of Xing [17] and Fu[18], the threshold value of ACT was determined as 3 s.

C. Generalized Extreme Value (GEV) Model Development

To model the crash risk, ACT was selected as the primary conflict indicator. Common safety indicators used to establish extreme crash risk models include TTC, PET, and MTTC[18-21]. These indicators, when less than 0 in value, imply the occurrence of an accident. ACT shares this property, and additionally, ACT is capable of reflecting conflict involving lane changing[22], which meets the requirements of our study.

The prerequisite for using EVT for crash risk calculation is that the occurrence of extremely small ACTs must be adequately modeled so that the probability of a crash can be derived[23]. Therefore, it is crucial to decide how to select the extremes. There are two common ways: Block Maxima (BM) and Peak over Threshold (POT). A number of studies have shown that the threshold selection in POT model is a major challenge, and it's hard to address the issue of serial dependence[24]. It's important to note that the EVT presupposes that the extreme value samples used for modeling adhere to independent and identically distributed conditions. Given the use of partitioned block sampling for extreme values, the BM method inherently addresses this issue during the process of parameter estimation, as noted in previous studies[23, 24]. In addition, small ACTs are rare events that also matches the adaptability of BM. Therefore, the BM model is used for this study.

The BM model involves dividing the data into blocks at certain intervals and selecting the block maximums to fit the GEV distribution. The k_{th} largest sample in a set of independent identically distributed samples in a block can be denoted as:

$$M_n^{(k)} = k_{th}\ largest\ of\ \{X_1, X_2, \dots, X_n\} \tag{5}$$

Where, X_i represents the sample observation and $M_n^{(k)}$ denotes the k_{th} largest sample observation within a block. When n tends to infinity, for the first k largest samples, their joint probability density function is (for $\xi \neq 0$).

$$s^{(r)} = \frac{x^{(r)} - \mu}{\sigma} \tag{6}$$

$$f(x^{(1)}, \dots, x^{(r)}) = exp\left\{-[1 + \xi \times s^{(r)}]^{-\frac{1}{\xi}}\right\} \times \prod_{k=1}^{r} \sigma^{-1}[1 + \xi \times s^{(r)}]^{-\frac{1}{\xi}-1} \tag{7}$$

where the location (μ), scale (σ), and shape parameters (ξ) of the equation need to satisfy $\sigma > 0$, and μ and ξ are real

number; and $x^{(r)} \leq x^{(r-1)} \leq \cdots \leq x^{(1)}$; and $x^{(k)}: 1 + \xi \times s^r > 0$ for k=1,2,…,r.

Similar to previous studies that used driving data to develop extreme value models to assess the crash risk[21, 24, 25]，this study also the MLCS of each driver as a block. Therefore, the duration of each block varies depending on the MLCS duration. In order to get enough extreme values for modeling, instead select only one sample in each block, we use the smallest r ACTs from each block. To ensure the r ACTs represent the real dangerous situation, only ACTs below 3s are selected[21, 26-29]. Then, to decide the optimum r value, we used Akaike information criterion (AIC) and Bayesian Information criterion (BIC)[23, 24].

Two kinds of GEV models, a stationary model and non-stationary models are built separately for both ACPs. A stationary model is a GEV model without other covariates. And the non-stationary GEV models are the models with other covariates. In non-stationary GEV models, we integrated covariates into the GEV model's location parameter (μ) via the identity link function[22, 24, 30], as outlined in the following mathematical expression.

$$\mu_i = \mu_0 + \boldsymbol{\beta Y} \tag{8}$$

where μ_i denotes the location parameter of the GEV model, $\boldsymbol{\beta}$ denotes the estimated coefficients of the covariates, and $\boldsymbol{Y}$ denotes the covariates added to the model.

Similar to the method of finding the optimum r, AIC and BIC are used to find the best combinations of the covariates for non-stationary GEV models, and the models with smaller AIC/BIC are preferred.

As previously state, ACT is the main variable for GEV modeling. When a pair of vehicles do not approach each other, the ACT value is positive infinity. Otherwise, ACT is a positive real number. Similar to TTC, a smaller ACT represents a higher risk, and a hypothetical ACT which is zero or less than zero can represent a collision. Because the GEV is only applicable to the largest values within the blocks, we need to add a negative sign to ACT so that the ACT values represent higher risk will be captured by the GVT model [12, 21, 23, 24, 27, 31]. Thus, the probability of a crash is converted to the probability of a negative ACT greater than or equal to zero, and the mathematical form is expressed as follows.

$$R = P(Z \geq 0) = 1 - G(0) \tag{9}$$

where, R and Z denote the risk of collision and the maximum negative ACT respectively, and G (·) is the fitted GEV distribution.

III. Results

A. GEV Model Results

Following the computation of AIC and BIC for non-stationary models incorporating different combination of covariates across a range of r values (from 1 to 8), the optimal r value was established as 5. After the r is set to 5, the best set of covariates are decided as D2R, speed, DPC, DRAC, and TE-ACT. Then, to establish a foundation for comparison, we also constructed stationary models to serve as our baseline.

Evidence of the accuracy of our model selection between stationary and non-stationary models came from the likelihood-ratio test results (see TABLE I). These showed that introducing covariates to the location parameters of PFO and PBE led to significantly better model fits compared to stationary models. This improvement was statistically significant with a p-value less than 0.001, indicating that our results are valid at a 95% confidence level. displays kernel probability density plots of the best non-stationary for PFO and PBE. Upon examination of these kernel probability density plots, we found a close alignment between the fitted model and empirical data.

TABLE I. FITTING EFFECT (AIC AND BIC) OF STATIONARY MODEL AND BEST NON-STATIONARY MODEL

Model	AIC	BIC	Likelihood-ratio Test
Stationary PBE model	185	192	P<0.05
Best non-stationary PBE model	-54	-36	
Stationary PFO model	123	129	P<0.05
Best non-stationary PFO model	-1	15	

The structure of the data and the statistical summary are shown in TABLE II. Given the nature of these variables, Max(-ACT), speed, acceleration, D2R, DPC,DRAC are all instant data that is corresponding to a specific time point and indicate the state of the HDV. Acceleration noise and TE-ACT are the process variables measuring the process during MLCS. Therefore, their values won't change in the same MLCS. DR is the scenario level variable that indicates the initial condition of a scenario. DR won't change in the same scenario.

The optimal non-stationary models identified for both EMCs share the same set of covariates: D2R, speed, DPC, DRAC, and TE-ACT as shown in TABLE III. In our model, we assume that the scale and shape parameters are not changing with covariates. These covariates directly influence the location parameters of the GEV distribution, which in turn affect the crash risk. As such, the location parameter serves as a critical determinant of crash risk: a larger location parameter corresponds to a higher expected number of crashes[19].

TABLE II. THE STATISTICAL SUMMARY OF THE VARIABLES

Variables	Level	PFO Mean		PBE Mean	
		Mean	*S.D.*	*Mean*	*S.D.*
Max(-ACT) (r=5)	Instant (main)	-1.85	0.79	-1.65	0.88
Speed (Km/h)	Instant	110.99	19.04	13.43	13.10
Acceleration (m/ss)	Instant	0.17	1.02	-4.79	2.97
D2R (m)	Instant	245.70	180.26	276.68	284.87
DPC (m)	Instant	-45.67	8.76	39.62	26.07
DRAC (m/ss)	Instant	2.50	9.77	6.55	12.04
Acceleration Noise (m/ss)	MLCS	0.79	0.52	3.30	0.53
TE-ACT (s)	MLCS	0.86	0.64	1.83	1.25
DR (m)	Scenario	556.60	159.94	468.06	165.15

For both models, three out of five coefficients share the same sign: D2R, DRAC, and TE-ACT. The D2R coefficient is negative, indicating that a decrease in the D2R shifts the GEV distribution to the right, enlarges the area greater than 0, and exacerbates the crash risk. This finding is consistent with existing studies[14, 24, 32]. A possible explanation is that as the D2R diminished, drivers' motivation to bypass the platoon and enter the ramp strengthened, leading to more intense

maneuvers, and thereby increasing driving risk. A higher DRAC value is associated with a higher crash risk, which is consistent with previous studies[33, 34]. It's worth noting that the DRAC coefficient for the PBE model is larger than that for the PFO model. This possibly because the main risk of PEB is from the rear vehicle, which is more sensitive to DRAC. In our model, this coefficient of TE-ACT is positive, implying that prolonged exposure to the hazardous condition during the mandatory lane change increases the location parameter and thus, the crash risk.

The speed variable coefficients display contrasting signs for the two models. Within the context of PBE, a negative sign for the speed coefficient suggests that lower speeds correspond to a higher location parameter, thus indicating an increased crash risk. This aligns with intuition as a slower MV choosing to decelerate during the implies a shorter ACT with the Rear Vehicle (RV). Concerning PFO, the problem becomes two-dimensional, entailing both speed and the angle between two vehicles. Consequently, direct positive sign determination proves difficult. Nevertheless, several studies on MLCS [24, 25] concur that higher speed correlates with increased crash risk. Lastly, DPC coefficients also exhibit contrary signs. For PFO, an increase in DPC aligns with an increased location parameter, suggesting that as the distance from the center of the HTP grows, the likelihood of extreme ACT occurrences and thus driving risk, increases. Conversely, for PBE, a smaller DPC means a higher location parameter, signifying that proximity to the center of the platoon increases the potential for hazardous ACTs and thereby elevates driving risk. This may be related to the evading target of the MV. For PFO, MV needs to overtake the head of the HTP and for PBE, MV needs to evade the tail of the HTP. Longer distance between the MV and the evading targe increases the crash risk.

TABLE III. THE PARAMETERS OF THE PFO AND PBE MODELS

Model	Location μ						Scale σ	Shape ξ
	μ_0	μ_{D2R}	μ_{speed}	μ_{DPC}	μ_{DRAC}	μ_{TE-ACT}		
PFO	-4.18	-0.0003	0.03	0.0004	0.003	1.37	0.11	0.90
PBE	-1.73	-0.0001	-0.11	-0.0014	0.014	0.140	0.07	1.06

B. *Scenario Crash Risk Analysis*

In the experimental design, the only changing variables among different scenarios is DR, short (300m, 400m), medium (500m, 600m), long (700m, 800m). The estimated crash risk for each scenario was calculated by employing the mean value (in TABLE IV) of the covariates in each specific context.

TABLE IV. THE MEAN VALUE OF VARIABLES IN THE FINAL MODELS

Variables	Short Scenario		Medium Scenario		Long Scenario	
	PFO	*PBE*	*PFO*	*PBE*	*PFO*	*PBE*
Max(-ACT) (s)	-1.23	-1.33	-2.01	-2.16	-2.22	-1.87
Speed (km/h)	95.33	10.99	120.02	19.40	112.75	9.97
Acceleration (m/s^2)	-0.81	-3.79	-0.51	-5.55	0.62	-6.50
D2R (m)	77.18	175.32	191.87	501.19	496.78	270.80
DPC (m)	-41.70	44.33	-46.02	42.08	-36.01	42.20
DRAC (m/s^2)	8.28	9.61	0.25	2.53	0.17	3.42
TE-ACT (s)	1.27	2.24	0.66	1.19	0.77	1.53

For PFO, the crash risk in the three scenarios are as follows: 0.051 in the short scenario, 0.036 in the medium scenario, and 0.035 in the long scenario. An evident trend emerges where the crash risk diminishes as the DR increases, particularly transitioning from short to medium scenarios. This observation underscores that extending the critical DR can significantly mitigate crash risk. As for PBE, the crash risks across scenarios are 0.044 (short), 0.035 (medium), and 0.041 (long). Although we cannot conclude that an increase in DR effectively decrease the crash risk, when the DR shift from short to any other scenario, the crash risk decreases. Both results of PFO and PBE highlights the importance to reduce risk by providing HDV a relatively large DR value.

Furthermore, the comparison of the EMCs in the same scenario are shown in Figure 4. it's noteworthy that in the short scenario, the crash risk for PFO is higher, while in the medium scenario, the crash risk for both ACPs is roughly equal. Interestingly, the long scenario sees PBE as the riskier behavior. This counter-intuitive result could potentially be attributed to the driver's ability to switch evasion maneuvers. With a longer DR, drivers have additional time to select their EMCs. However, some drivers might initially opt for PFO, but due to insufficient acceleration or the prolonged nature of the process, they may realize that the D2R could become inadequate. Consequently, they switch to PBE. This extended process of changing strategies may inadvertently increase the associated risk, leading to the heightened crash risk observed in the long scenario for PBE.

In the short scenario, overtaking the HTP to access the off-ramp posed a high risk, with several drivers displaying serious traffic violations (such as speeding or crossing a solid line to enter the ramp). However, as the DR lengthened (long scenario), the act of overtaking became markedly less hazardous. Similar patterns were noted for PBE. In addition, during the experiments, some drivers obstructed from seeing the off-ramp by the HTP would execute sharp deceleration maneuvers even when sufficient distance for a smoother slowdown was available.

One of the most direct implications of these findings is the regulation of evasion maneuver choices based on the distance to the ramp (D2R). For instance, in situations similar to the study, a platoon front overtaking is not permitted when the D2R is short (e.g., < 400 m).

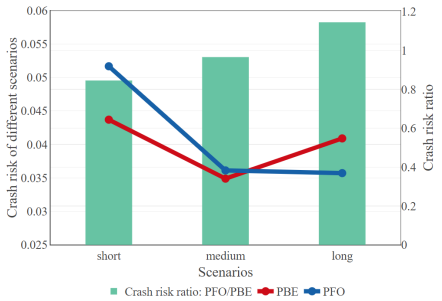

Figure 4. Crash risk of PFO and PBE in different scenarios.

ACKNOWLEDGMENT

The presented work in this paper is partially supported by C2SMART, a Tier 1 University Transportation Center at New York University, Sichuan Science and Technology Program (2021YJ0042), and the Key Laboratory of Road and Traffic Engineering of the Ministry of Education, Tongji University

(K202001). The contents of this paper only reflect the views of the authors who are responsible for the facts and do not represent any official views of the sponsoring organizations.

REFERENCES

[1] G. Jornod, A. Pfadler, S. Carreira, A. El Assaad, and T. Kürner, "Fuel Efficient High-Density Platooning Using Future Conditions Prediction," *IEEE Open Journal of Intelligent Transportation Systems,* vol. 3, pp. 786-798, 2022.

[2] S. Calvert, W. J. Schakel, and B. van Arem, "Evaluation and modelling of the traffic flow effects of truck platooning," *Transportation research part C: emerging technologies,* vol. 105, pp. 1-22, 2019.

[3] S. Tsugawa, S. Jeschke, and S. E. Shladover, "A Review of Truck Platooning Projects for Energy Savings," *IEEE Transactions on Intelligent Vehicles,* vol. 1, no. 1, pp. 68-77, 2016, doi: 10.1109/TIV.2016.2577499.

[4] A. Ghosal *et al.*, "Truck platoon security: State-of-the-art and road ahead," *Computer Networks,* vol. 185, p. 107658, 2021.

[5] B. Chen, D. Sun, J. Zhou, W. Wong, and Z. Ding, "A future intelligent traffic system with mixed autonomous vehicles and human-driven vehicles," *Information Sciences,* vol. 529, pp. 59-72, 2020.

[6] Y. Guo, Z. Li, and T. Sayed, "Analysis of crash rates at freeway diverge areas using bayesian tobit modeling framework," *Transportation research record,* vol. 2673, no. 4, pp. 652-662, 2019.

[7] Y. Lu, K. Cheng, Y. Zhang, X. Chen, and Y. Zou, "Analysis of lane-change conflict between cars and trucks at merging section using UAV video data," *arXiv preprint arXiv:.07881,* 2022.

[8] Y. Ying, S. Yan-ting, Y. Hua-zhi, and L. Hao-xue, "Driving risk evaluation and speed control in passageway areas of freeway," *Journal of T raffic and T ransportation Engineering,* vol. 11, no. 02, pp. 90-96, 2011, doi: 10.19818/j.cnki.1671-1637.2011.02.015.

[9] S. Santini, A. Salvi, A. S. Valente, A. Pescapé, M. Segata, and R. L. Cigno, "A consensus-based approach for platooning with intervehicular communications and its validation in realistic scenarios," *IEEE Transactions on Vehicular Technology,* vol. 66, no. 3, pp. 1985-1999, 2016.

[10] A. Papadoulis, M. Quddus, and M. Imprialou, "Evaluating the safety impact of connected and autonomous vehicles on motorways," *Accident Analysis & Prevention,* vol. 124, pp. 12-22, 2019.

[11] Y. Li, Y. Tu, Q. Fan, C. Dong, and W. Wang, "Influence of cyber-attacks on longitudinal safety of connected and automated vehicles," *Accident Analysis & Prevention,* vol. 121, pp. 148-156, 2018.

[12] M. Gouy, C. Diels, N. Reed, A. Stevens, and G. Burnett, "Do drivers reduce their headway to a lead vehicle because of the presence of platoons in traffic? A conformity study conducted within a simulator," *IET Intelligent Transport Systems,* vol. 7, no. 2, pp. 230-235, 2013.

[13] M. Gouy, K. Wiedemann, A. Stevens, G. Brunett, N. Reed, and behaviour, "Driving next to automated vehicle platoons: How do short time headways influence non-platoon drivers' longitudinal control?," *Transportation research part F: traffic psychology,* vol. 27, pp. 264-273, 2014.

[14] S. Razmi Rad, H. Farah, H. Taale, B. van Arem, and S. P. Hoogendoorn, "The impact of a dedicated lane for connected and automated vehicles on the behaviour of drivers of manual vehicles," *Transportation Research Part F: Traffic Psychology and Behaviour,* vol. 82, pp. 141-153, 2021/10/01/ 2021, doi: https://doi.org/10.1016/j.trf.2021.08.010.

[15] S. P. Venthuruthiyil and M. Chunchu, "Anticipated Collision Time (ACT): A two-dimensional surrogate safety indicator for trajectory-based proactive safety assessment," *Transportation Research Part C: Emerging Technologies,* vol. 139, p. 103655, 2022/06/01/ 2022, doi: https://doi.org/10.1016/j.trc.2022.103655.

[16] L. Yue, M. Abdel-Aty, Z. J. J. o. I. Wang, and C. Vehicles, "Effects of connected and autonomous vehicle merging behavior on mainline human-driven vehicle," 2021.

[17] X. Qu, Y. Yang, Z. Liu, S. Jin, and J. Weng, "Potential crash risks of expressway on-ramps and off-ramps: A case study in Beijing, China," *Safety Science,* vol. 70, pp. 58-62, 2014/12/01/ 2014, doi: https://doi.org/10.1016/j.ssci.2014.04.016.

[18] C. Fu and T. Sayed, "Bayesian dynamic extreme value modeling for conflict-based real-time safety analysis," *Analytic methods in accident research,* vol. 34, p. 100204, 2022.

[19] L. Zheng and T. Sayed, "Bayesian hierarchical modeling of traffic conflict extremes for crash estimation: A non-stationary peak over threshold approach," *Analytic Methods in Accident Research,* vol. 24, p. 100106, 2019/12/01/ 2019, doi: https://doi.org/10.1016/j.amar.2019.100106.

[20] L. Zheng, T. Sayed, and A. Tageldin, "Before-after safety analysis using extreme value theory: A case of left-turn bay extension," *Accident Analysis & Prevention,* vol. 121, pp. 258-267, 2018/12/01/ 2018, doi: https://doi.org/10.1016/j.aap.2018.09.023.

[21] H. Farah and C. L. Azevedo, "Safety analysis of passing maneuvers using extreme value theory," *IATSS Research,* vol. 41, no. 1, pp. 12-21, 2017/04/01/ 2017, doi: https://doi.org/10.1016/j.iatssr.2016.07.001.

[22] P. Kar, S. P. Venthuruthiyil, and M. Chunchu, "Assessing the crash risk of mixed traffic on multilane rural highways using a proactive safety approach," *Accident Analysis & Prevention,* vol. 188, p. 107099, 2023/08/01/ 2023, doi: https://doi.org/10.1016/j.aap.2023.107099.

[23] L. Zheng, K. Ismail, and X. Meng, "Freeway safety estimation using extreme value theory approaches: A comparative study," *Accident Analysis & Prevention,* vol. 62, pp. 32-41, 2014/01/01/ 2014, doi: https://doi.org/10.1016/j.aap.2013.09.006.

[24] Y. Ali, M. M. Haque, and Z. Zheng, "Assessing a Connected Environment's Safety Impact During Mandatory Lane-Changing: A Block Maxima Approach," *IEEE Transactions on Intelligent Transportation Systems,* 2022.

[25] Y. Ali, M. M. Haque, and Z. Zheng, "An Extreme Value Theory approach to estimate crash risk during mandatory lane-changing in a connected environment," *Analytic Methods in Accident Research,* vol. 33, p. 100193, 2022/03/01/ 2022, doi: https://doi.org/10.1016/j.amar.2021.100193.

[26] C. Fu, T. Sayed, and L. Zheng, "Multi-type Bayesian hierarchical modeling of traffic conflict extremes for crash estimation," *Accident Analysis & Prevention,* vol. 160, p. 106309, 2021/09/01/ 2021, doi: https://doi.org/10.1016/j.aap.2021.106309.

[27] C. Fu and T. Sayed, "Random parameters Bayesian hierarchical modeling of traffic conflict extremes for crash estimation," *Accident Analysis & Prevention,* vol. 157, p. 106159, 2021/07/01/ 2021, doi: https://doi.org/10.1016/j.aap.2021.106159.

[28] L. Xing, J. He, M. Abdel-Aty, Y. Wu, and J. Yuan, "Time-varying Analysis of Traffic Conflicts at the Upstream Approach of Toll Plaza," *Accident Analysis & Prevention,* vol. 141, p. 105539, 2020/06/01/ 2020, doi: https://doi.org/10.1016/j.aap.2020.105539.

[29] T. Zhang and K. Gao, "Will Autonomous Vehicles Improve Traffic Efficiency and Safety in Urban Road Bottlenecks? The Penetration Rate Matters," in *2020 IEEE 5th International Conference on Intelligent Transportation Engineering (ICITE)*, 11-13 Sept. 2020 2020, pp. 366-370, doi: 10.1109/ICITE50838.2020.9231360.

[30] Y. Guo, T. Sayed, L. Zheng, and M. Essa, "An extreme value theory based approach for calibration of microsimulation models for safety analysis," *Simulation Modelling Practice and Theory,* vol. 106, p. 102172, 2021/01/01/ 2021, doi: https://doi.org/10.1016/j.simpat.2020.102172.

[31] F. Orsini, G. Gecchele, M. Gastaldi, and R. Rossi, "Collision prediction in roundabouts: a comparative study of extreme value theory approaches," *Transportmetrica A Transport Science,* vol. 15, no. 2, pp. 556-572, 2019/01/01/ 2019, doi: https://doi.org/10.1080/23249935.2018.1515271.

[32] Y. Ali, M. M. Haque, Z. Zheng, S. Washington, and M. Yildirimoglu, "A hazard-based duration model to quantify the impact of connected driving environment on safety during mandatory lane-changing," *Transportation research part C: emerging technologies,* vol. 106, pp. 113-131, 2019.

[33] D. Shah and C. Lee, "Analysis of effects of driver's evasive action time on rear-end collision risk using a driving simulator," *Journal of Safety Research,* vol. 78, pp. 242-250, 2021/09/01/ 2021, doi: https://doi.org/10.1016/j.jsr.2021.06.001.

[34] C. Fu and T. Sayed, "Comparison of threshold determination methods for the deceleration rate to avoid a crash (DRAC)-based crash estimation," *Accident Analysis & Prevention,* vol. 153, p. 106051, 2021/04/01/ 2021, doi: https://doi.org/10.1016/j.aap.2021.106051.